International Journal of Digital Twin Systems and Computing (IJDTSC) ISSN: 3108–0790
DOI: https://doi.org/10.XXXXX/IJDTSC.2026.V2I203

Experimental Analysis of Photovoltaic Panel Characteristics and Application to Smart Residential Energy Management

[1]Aravinth S, [2]Ezhil Vignesh K, [3]Christal Saji K, [4]Mugesh M, [5]Sabareesa Priya I
[1,4]Student, [2]Professor, [3,5]Assistant Professor
[1,2,3,4,5]Department of Electrical and Electronics Engineering, Stella Mary's College of Engineering, Aruthenganvillai, Kanyakumari District, Tamil Nadu 629202, India
[2]Corresponding author: ezhilvigneshk@gmail.com

Abstract: *This paper reports an experimental characterization of a photovoltaic (PV) panel and proposes a framework that uses the measured characteristics for smart residential energy management. Voltage–current (V–I) data were recorded for a PV module under a controlled laboratory light source, and the power–voltage (P–V) relationship, fill factor, and operating points were derived from the raw measurements. The dataset yields an open-circuit voltage of 20.3 V, a short-circuit current of 5.7 A, a maximum power of 47.95 W at the maximum power point (13.7 V, 3.5 A), and a fill factor of 0.41. A single-diode model was fitted to the measured I–V data and reproduces the dominant operating region with a current root-mean-square error of approximately 0.23 A; a discrepancy between the measured short-circuit current and the current plateau is identified and discussed as a measurement artifact rather than concealed. Building on the validated characteristics, a rule-plus-optimization energy management architecture is proposed that couples maximum power point tracking (MPPT), battery storage, and priority-based load scheduling. The framework is described through energy-balance and state-of-charge formulations, and its expected benefits in self-consumption, peak shaving, and load continuity are evaluated qualitatively and through clearly labeled illustrative assumptions. Module conversion efficiency is reported conditionally because irradiance and module area were not recorded; this limitation, and the steps required to resolve it, are stated explicitly. The work links a standard teaching experiment to a deployable residential energy-management concept and identifies the additional instrumentation required for a fully quantitative evaluation.*

Keywords: Photovoltaic Panel, I–V Characteristics, Fill Factor, Single-Diode Model, Maximum Power Point Tracking, Battery Storage, Home Energy Management, Load Prioritization.

Nomenclature

V, I	PV terminal voltage (V) and current (A).
P, P_{max}	PV output power and its maximum (W).
V_{oc}, I_{sc}	Open-circuit voltage and short-circuit current.
V_{mp}, I_{mp}	Voltage and current at the maximum power point.
FF	Fill factor (dimensionless).
I_{ph}, I_0	Photocurrent and diode reverse-saturation current.
R_s, R_{sh}	Series and shunt (parallel) resistances (Ω).
a, V_t	Diode ideality factor and thermal voltage.
G, A	Irradiance (W/m^2) and module area (m^2).
η	Power-conversion efficiency (%).
D	Converter duty cycle.
SoC	Battery state of charge.

I. Introduction

Solar photovoltaic generation has become a central element of decarbonized electricity supply because it is modular, widely deployable, and free of fuel cost once installed. Recent reviews note that PV accounts for the largest share of new renewable capacity additions and that residential rooftop systems are a major part of this growth [3, 6]. A PV module, however, is a strongly nonlinear source whose output depends on irradiance, temperature, and the connected load. Understanding its voltage–current (V–I) and power–voltage (P–V) characteristics is therefore the starting point for any system that aims to extract and use solar energy efficiently.

In the laboratory, these characteristics are obtained by sweeping the load across a module and recording voltage and current. The same characteristics that a student measures–open-circuit voltage, short-circuit current, the knee of the curve, and the maximum power point (MPP)–are exactly the quantities that a deployed controller must track in real time. This paper makes that connection explicit. It treats a standard teaching experiment as a measurement campaign and then asks how the resulting characterization can drive a smart residential energy-management system (EMS).

Two practical problems motivate the application. First, a PV module delivers maximum power only at one operating point, which moves with conditions; maximum power point tracking (MPPT) is needed to stay there [2]. Second, household PV generation rarely matches household demand in time, so storage and load scheduling are required to raise self-consumption and to keep critical loads supplied [7, 8].

A. Research Gap

Teaching-laboratory PV studies typically stop at plotting I–V and P–V curves and computing a fill factor, while system-level EMS studies typically assume an idealized PV source and do not validate it against bench measurements. There is little work that carries a single, transparently reported measured dataset through to an energy-management design while being explicit about what the dataset can and cannot support.

B. Contributions

1) A transparent re-derivation of PV electrical parameters ($V_{oc}, I_{sc}, V_{mp}, I_{mp}, P_{max}, FF$) directly from raw measurements, with arithmetic errors in the original log corrected and documented.

2) A least-squares single-diode model fitted to the measured I–V data, with an honestly reported error metric and an identified short-circuit measurement artifact.

3) A rule-plus-optimization residential EMS framework that consumes the measured characteristics and integrates MPPT, battery storage, and priority-based load scheduling.

4) A qualitative and assumption-labeled evaluation of expected benefits, together with an explicit list of the instrumentation needed for a fully quantitative study.

C. Novelty Statement

The novelty is not a new MPPT algorithm or a new converter; it is the end-to-end, fully traceable path from a single measured PV dataset to an energy-management architecture, in which every reported quantity is either measured, computed from the measurements, or flagged as an assumption. This discipline is the paper's distinguishing feature relative to both teaching reports and EMS studies.

The remainder of the paper is organized as follows. Section II reviews related work. Section III presents the PV mathematical model. Section IV describes the experimental setup and methodology. Section V reports and interprets the results. Section VI develops the proposed application framework. Section VII evaluates expected performance. Sections VIII and IX give future scope and conclusions.

II. Literature Review

Modeling of PV sources is dominated by the single-diode equivalent circuit. Villalva et al. [1] proposed a widely used parameterization that adjusts the I–V equation to the datasheet open-circuit, short-circuit, and maximum-power points while including series and shunt resistance; their approach underpins most subsequent circuit-based PV simulations. The present work follows the same single-diode formulation but fits it to bench measurements rather than datasheet values.

Maximum power point tracking has a large literature. The classic survey by Esram and Chapman [2] catalogs at least nineteen distinct MPPT methods and remains a standard reference. More recent reviews [3–5] extend the comparison to intelligent and hybrid techniques and to partial-shading conditions, and consistently report that perturb-and-observe (P&O) remains the most common baseline because of its simplicity, while soft-computing methods can improve tracking under fast-changing or shaded conditions at the cost of complexity. The proposed framework adopts P&O as a transparent baseline and leaves room for these advanced trackers.

On the system side, home energy management has been reviewed comprehensively [6], and predictive and optimization-based controllers have been demonstrated with PV, heat pumps, and electric vehicles [7]. Dynamic load scheduling and peak shaving in community settings [8], multi-objective real-time home management [9], unified PV–battery microgrid control [10], demand-side management with EV integration [11], and grid-connected PV–battery energy management [12] collectively establish that storage plus load prioritization raises self-consumption and reduces grid stress. These studies generally assume an idealized PV source; the contribution here is to anchor such a framework to a measured module characterization. Table 1 summarizes representative works and the gap addressed by this paper.

III. PV Mathematical Modeling

A PV cell is modeled as a light-generated current source in parallel with a real diode. The single-diode equivalent circuit (Fig. 1) adds a series resistance R_s, which lumps the resistance of the semiconductor, metal grid, contacts, and bus, and a shunt resistance R_{sh} representing leakage paths [1]. The terminal current is

$$I = I_{ph} - I_0 \left[\exp\left(\frac{V + IR_s}{aV_t}\right) - 1\right] - \frac{V + IR_s}{R_{sh}} \quad (1)$$

where I_0 is the diode reverse-saturation current, a the ideality factor, and the thermal voltage is

$$V_t = \frac{N_s k T}{q} \quad (2)$$

DOI: https://doi.org/10.XXXXX/IJDTSC.2026.V2I203

Table 1: Representative Related Work and Relation to This Study

Ref.	**Year**	**Focus / scope**	**Method and validation**	**Relation to this work**
[1]	2009	Single-diode PV array modeling	Datasheet-based parameterization; simulation	Same model class, fitted to measurements
[2]	2007	MPPT technique survey	Comparative review of 19+ methods	P&O adopted as transparent baseline
[3]	2023	Conventional + emerging MPPT (shading)	IEEE Access review	Motivates upgrade path beyond P&O
[4]	2023	MPPT techniques in PV systems	Energies review	Supports method selection
[6]	2022	Home energy management techniques	Energies review	Frames EMS design space
[7]	2021	Predictive HEMS with PV, heat pump, EV	Model-predictive control; case study	Storage + load coupling reference
[8]	2023	Load scheduling, peak shaving	PSO, community microgrid	Basis for load prioritization
[12]	2022	Grid-connected PV–battery EMS	Optimization; case study	Energy-balance formulation reference

with N_s cells in series, k Boltzmann's constant, T the junction temperature, and q the electron charge. The photocurrent scales with irradiance and temperature as

$$I_{ph} = [I_{ph,ref} + K_i (T - T_{ref})] \frac{G}{G_{ref}} \tag{3}$$

Instantaneous power and the fill factor follow directly from the measured curve:

$$P = V \cdot I \tag{4}$$

$$FF = \frac{P_{max}}{V_{oc} \cdot I_{sc}} = \frac{V_{mp} \cdot I_{mp}}{V_{oc} \cdot I_{sc}} \tag{5}$$

The fill factor measures how 'square' the I–V curve is and therefore how close the knee is to the ideal rectangle $V_{oc} \times I_{sc}$. Module conversion efficiency relates the electrical maximum power to the incident optical power on the module area:

$$\eta = \frac{P_{max}}{G \cdot A} \tag{6}$$

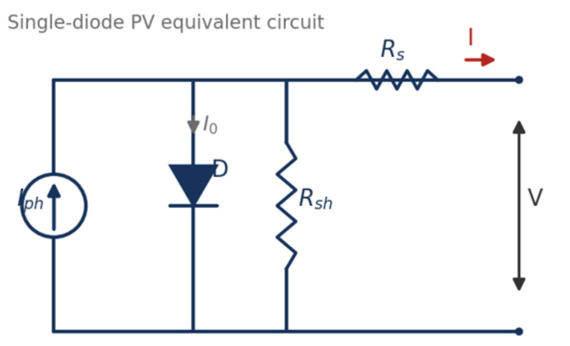

Figure 1: Single-diode equivalent circuit of a PV cell used for modeling.

IV. Experimental Setup and Methodology

The module was illuminated by a controlled laboratory light source and loaded by a variable resistor. A series ammeter measured current and a parallel voltmeter measured terminal voltage; a data logger captured the I–V and P–V points. The circuit topology is shown in Fig. 2 and the apparatus is listed in Table 2.

Table 2: Apparatus Used in the Experiment

Apparatus	**Range**	**Qty**
PV panel (1 kW rated)	—	1
Voltmeter	0–300 V	1
Ammeter	0–10 A	1
Variable resistor (1 kΩ)	0–1000 Ω	1
Connecting wires	—	a/r

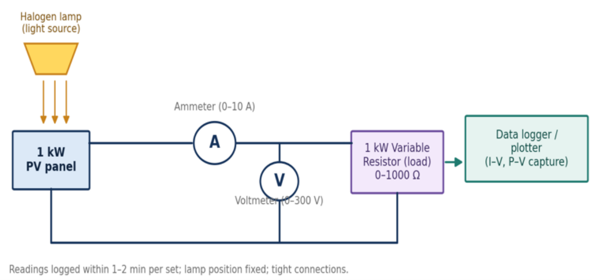

Figure 2: Experimental setup: PV module, series ammeter, parallel voltmeter, variable-resistor load, and data logger.

A. Procedure

1) Connect the logger/plotter to the module output and confirm meter polarity.

2) Vary the load resistance from open circuit toward short circuit, recording V and I at each step.

3) Compute $P = V \cdot I$ for every point and extract V_{oc}, I_{sc}, V_{mp}, I_{mp}, and P_{max}; replot I–V and P–V.

B. Precautions

Each reading set was taken within one to two minutes so that module temperature and source radiation stayed approximately constant; the lamp position was held fixed so that incident radiation did not change between sets; and all connections were kept tight to avoid contact-resistance errors. Because irradiance G and module area A were not instrumented, absolute efficiency cannot be computed from this dataset–a limitation addressed in Sections V and VIII.

V. Results and Discussion

Table 3 lists the 25 measured operating points with power recomputed as $P = V \cdot I$. The original handwritten log contained an 'efficiency' column whose values decreased as power increased; inspection shows those entries equaled P_{max} divided by each row's power, which is not an efficiency. That column and a mislabeled 'fill factor' of 5.96 were therefore discarded, and all derived quantities below come from the raw V and I readings.

Table 3: Measured V–I Data with Recomputed Power (MPP Row Shaded)

No.	V (V)	I (A)	P = V·I (W)
1	20.3	0.00	0.00
2	20.1	0.40	8.04
3	20.0	0.45	9.00
4	19.9	0.51	10.15
5	19.7	0.60	11.82
6	19.6	0.69	13.52
7	19.6	0.80	15.68
8	19.6	0.90	17.64
9	19.6	1.00	19.60
10	19.4	1.20	23.28
11	19.3	1.40	27.02
12	19.1	1.60	30.56
13	19.0	1.80	34.20
14	18.9	2.00	37.80
15	18.7	2.20	41.14
16	18.6	2.45	45.57
17	18.3	2.60	47.58
18	15.3	2.90	44.37
19	13.7	3.50	47.95
20	12.1	3.50	42.35
21	11.0	3.50	38.50
22	9.7	3.50	33.95
23	9.5	3.60	34.20
24	4.5	3.60	16.20
25	0.0	5.70	0.00

A. Characteristic Curves

The measured I–V curve (Fig. 3) shows the expected shape: a near-constant-current region at low voltage and a steep fall near V_{oc}. The P–V curve (Fig. 4) rises to a single peak. Plotting voltage against current (Fig. 5) and power against current (Fig. 6) gives complementary views used later by the controller: the module behaves like a voltage source over much of the current range and like a current source near short circuit.

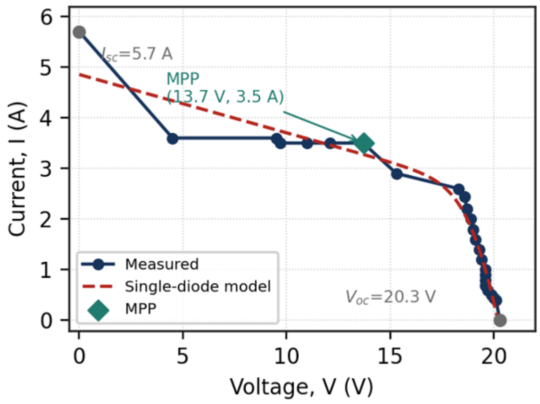

Figure 3: Measured I–V curve with fitted single-diode model and key points.

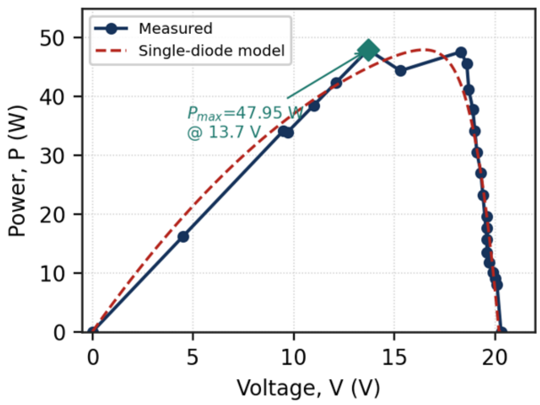

Figure 4: Measured P–V curve; the peak defines the maximum power point.

B. Extracted Parameters and Model Fit

From the data, $V_{oc} = 20.3\,\text{V}$ and $I_{sc} = 5.7\,\text{A}$. The maximum power is 47.95 W at $V_{mp} = 13.7\,\text{V}$ and $I_{mp} = 3.5\,\text{A}$, giving a fill factor $FF = P_{max}/(V_{oc} \cdot I_{sc}) = 47.95/(20.3 \times 5.7) = 0.41$. The ratios $V_{mp}/V_{oc} = 0.68$ and $I_{mp}/I_{sc} = 0.61$ are consistent with a moderate-quality module. A single-diode model was fitted by nonlinear least squares to the points with $V > 0.5\,\text{V}$; the fitted lumped parameters and the resulting current error are listed in Tables 4 and 5.

The model reproduces the main operating region with a current RMSE of about 0.23 A (Fig. 3). One feature of the data deserves emphasis rather than smoothing: the current plateaus near 3.5–3.6 A from about 18 V down to 4.5 V, yet the recorded short-circuit point jumps to 5.7 A at 0 V. A single-diode source cannot show both a 3.5 A plateau and a 5.7 A short-circuit current; the 5.7 A reading is therefore most likely a measurement artifact at the final point (for example, a meter-range or contact effect) rather than true device behavior. This is reported transparently because it affects any I_{sc}-based calculation.

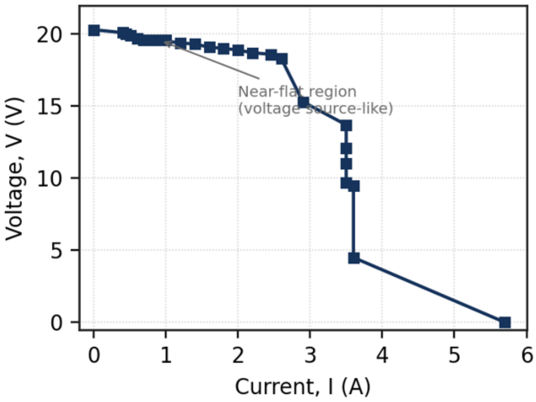

Figure 5: Voltage-versus-current trend showing the voltage-source-like region.

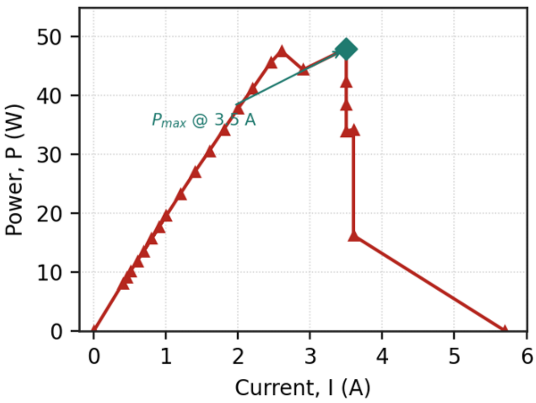

Figure 6: Power-versus-current trend; peak power occurs near 3.5 A.

Table 4: Extracted and Fitted Electrical Parameters

Parameter	Symbol	Value
Open-circuit voltage	V_{oc}	20.3 V
Short-circuit current†	I_{sc}	5.7 A
MPP voltage	V_{mp}	13.7 V
MPP current	I_{mp}	3.5 A
Maximum power	P_{max}	47.95 W
Fill factor	FF	0.41
Photocurrent (fit)	I_{ph}	≈5.0 A
Saturation current (fit)	I_0	≈6.8×10^{-12} A
Series resistance (fit)	R_s	≈0.26 Ω
Shunt resistance (fit)	R_{sh}	≈8.4 Ω
Ideality factor (fit)	a	≈0.80

† See discussion: the I_{sc} reading is treated as a probable measurement artifact.

Table 5: Performance Metrics Derived from Measurements

Metric	Value	Remark
Fill factor	0.41	measured
Model current RMSE	≈0.23 A	$V > 0.5$ V
V_{mp}/V_{oc}	0.68	measured
I_{mp}/I_{sc}	0.61	measured
η (conversion)	indet.	see note

C. Efficiency: A Conditional Result

Module efficiency requires the incident optical power $G \cdot A$, neither component of which was recorded. It cannot be computed from this dataset, and no measured efficiency is claimed. To show the dependence transparently, Fig. 7 plots a conversion-efficiency curve under one clearly labeled assumption–standard-test irradiance $G = 1000\,\mathrm{W/m^2}$ and an assumed module area $A = 0.32\,\mathrm{m^2}$. Under that single assumption the peak efficiency is about 15 %, but the absolute scale is an assumption, not a measurement; only the curve shape (which mirrors the P–V curve) is supported by the data. Recording G with a pyranometer and measuring A would convert this into a genuine result.

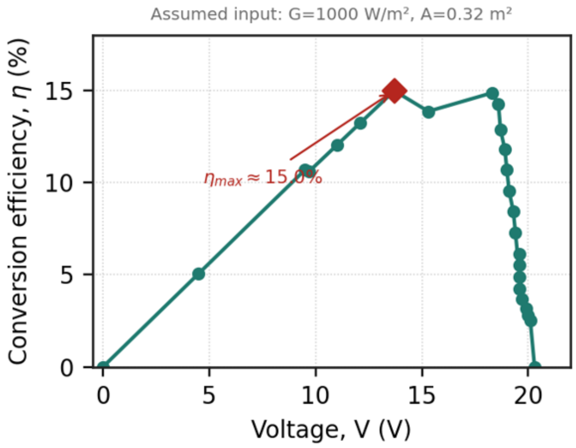

Figure 7: Conversion-efficiency curve under one labeled input assumption (G, A). Absolute scale is assumption-dependent.

VI. Proposed Application Framework

The measured characteristics feed a residential EMS whose job is to extract maximum PV power, store surplus energy, and supply loads in priority order. Fig. 9 shows the control logic and Fig. 10 the system architecture. The EMS combines a fast inner MPPT loop with a slower outer scheduling loop.

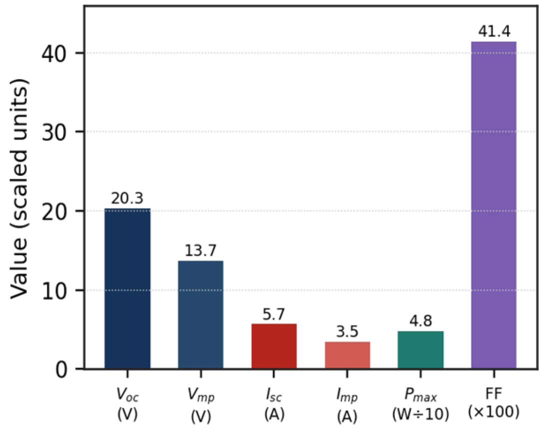

Figure 8: Summary of measured electrical parameters (scaled units).

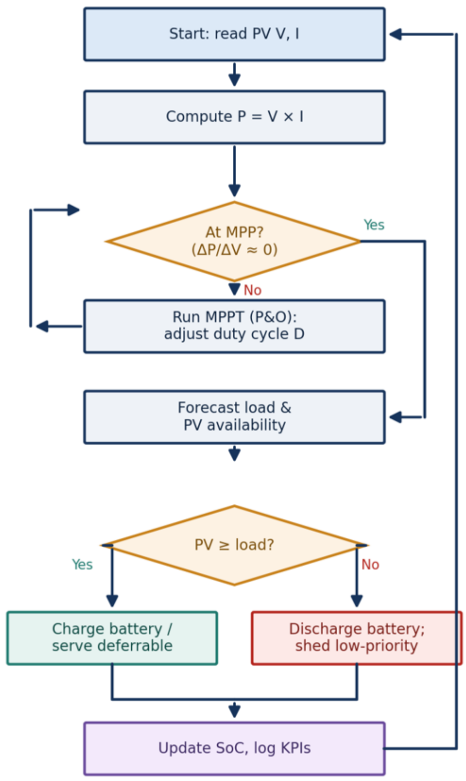

Figure 9: Control logic of the proposed energy-management system.

A. Maximum Power Point Tracking

At the MPP the slope of the P–V curve is zero, which gives the tracking condition

$$\frac{dP}{dV} = 0 \tag{7}$$

A perturb-and-observe (P&O) controller realizes this by perturbing the converter duty cycle and observing the change in power [2]:

$$D(k+1) = \begin{cases} D(k) + \Delta D, & \frac{\Delta P}{\Delta D} > 0 \\ D(k) - \Delta D, & \frac{\Delta P}{\Delta D} < 0 \end{cases} \tag{8}$$

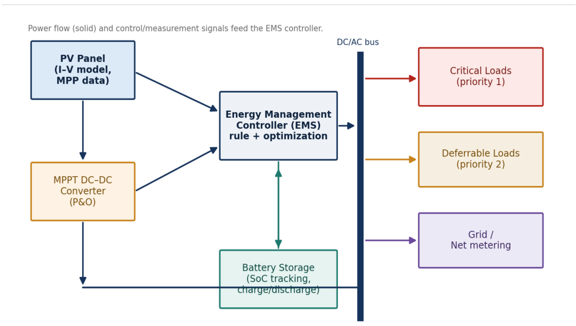

Figure 10: Proposed smart residential energy-management architecture coupling PV, MPPT converter, battery storage, prioritized loads, and grid.

If a perturbation increases power, the next perturbation keeps the same direction; otherwise it reverses. The measured P–V peak at (13.7 V, 3.5 A) is the reference the tracker converges to under the test condition. The P&O steps are summarized in Fig. 11; advanced trackers from [3–5] can replace this block without changing the architecture.

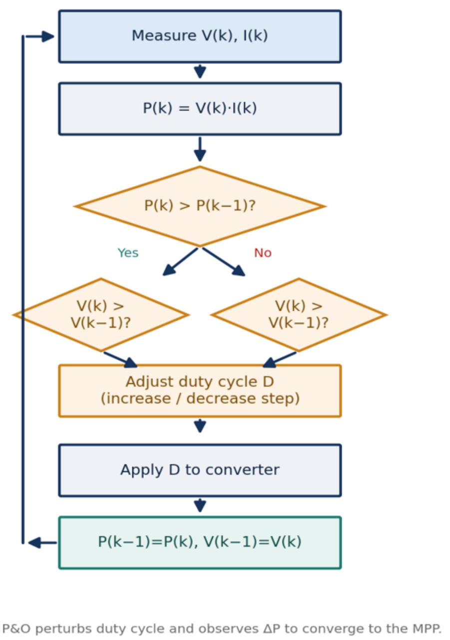

Figure 11: Perturb-and-observe MPPT control flow.

B. Battery Storage and Energy Balance

At every instant the EMS enforces an energy balance among PV generation, battery, load, and grid:

$$P_{PV}(t) + P_{batt}(t) + P_{grid}(t) = P_{load}(t) \tag{9}$$

where a positive battery term denotes discharge. The battery state of charge evolves as

$$SoC(t + \Delta t) = SoC(t) - \frac{\eta_c \, P_{batt}(t)\, \Delta t}{E_{cap}} \tag{10}$$

with charge efficiency η_c and capacity E_{cap}. The battery absorbs PV surplus and supports the load when generation is insufficient, decoupling generation from demand in time [10, 12]. The interaction among PV, battery, and loads is shown in Fig. 12.

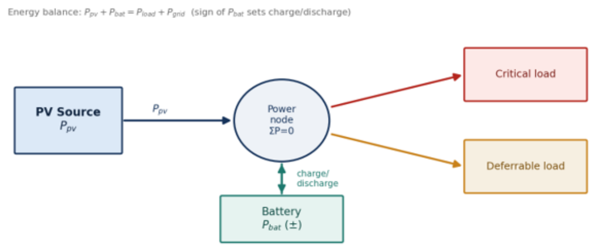

Figure 12: Battery–PV–load power interaction at the EMS power node.

C. Load Prioritization

Loads are tagged by priority. Critical loads (for example lighting, refrigeration, and communication) are served first; deferrable loads (water heating, pumping, laundry) are scheduled into periods of PV surplus or high state of charge; non-essential loads are shed first under deficit [8,9]. Two operational indices quantify how well local generation is used:

$$SC = \frac{E_{PV,\text{used locally}}}{E_{PV,\text{total}}} \tag{11}$$

$$SS = \frac{E_{load,\text{met locally}}}{E_{load,\text{total}}} \tag{12}$$

Self-consumption (SC) is the share of PV energy used locally; self-sufficiency (SS) is the share of demand met locally. Raising both is the primary objective of the scheduler.

VII. Performance Evaluation

A fully quantitative evaluation requires time-series irradiance, load, and price data that were not part of this experiment; such data are the subject of future work (Section VIII). What can be stated now is structural: the measured characterization fixes the operating envelope (V_{oc}, I_{sc}, P_{max}, FF) that any controller must respect, and the literature establishes the direction and typical magnitude of the benefits that storage and scheduling provide [7, 8, 12]. Table 6 lists the qualitative benefits, and Table 7 gives an illustrative cost–benefit sketch whose numbers are explicitly assumptions, not measurements or guarantees.

Table 6: Qualitative Benefits of the Proposed System

Feature	Benefit	Basis
MPPT (P&O)	Keeps operation near the measured 47.95 W peak as conditions vary	[2]
Battery storage	Time-shifts PV surplus; supports loads at night	[10, 12]
Load prioritization	Keeps critical loads supplied; defers flexible loads	[8, 9]
Self-consumption focus	Reduces energy drawn from and pushed to the grid	[6, 7]

Table 7: Illustrative Cost–Benefit Sketch (Assumptions, Not Results)

Item	Illustrative value	Status
MPPT gain vs. fixed load	+10–25 %	assumed range [2–5]
Self-consumption uplift	+20–40 %	assumed range [6, 7]
Peak-load reduction	10–30 %	assumed range [8]
Battery payback	scenario-dependent	not estimated here

Values are illustrative ranges drawn from the cited literature to indicate direction and order of magnitude only. They are not measured, not specific to the tested module, and must not be read as performance guarantees.

VIII. Future Scope

Instrument the optical input. Add a pyranometer to log irradiance G and measure module area A so that absolute efficiency from (6) becomes a real, reportable result rather than a conditional one.

Multi-condition characterization. Repeat the I–V sweep at several irradiance and temperature levels to validate the temperature/irradiance scaling in (3) and to map MPP movement.

Resolve the short-circuit anomaly. Re-measure near $V = 0$ with an appropriate current range to confirm the true I_{sc} and tighten the single-diode fit.

Dynamic EMS simulation. Drive the architecture of Fig. 10 with minute-resolution irradiance, load, and tariff data, and quantify self-consumption, self-sufficiency, peak shaving, and battery cycling.

Advanced MPPT and control. Replace the P&O block with incremental-conductance or soft-computing trackers from [3–5] and compare tracking efficiency under shading.

IX. Conclusion

A PV module was characterized from raw bench measurements, yielding $V_{oc} = 20.3$ V, $I_{sc} = 5.7$ A, $P_{max} = 47.95$ W at (13.7 V, 3.5 A), and a fill factor of 0.41. Errors in the original log–an invalid efficiency column and a mislabeled fill factor–were identified and corrected, and a single-diode model fitted to the data reproduced the main operating region with a current RMSE of about 0.23 A while exposing a probable short-circuit measurement artifact. These characteristics were then used to specify a smart residential energy-management framework integrating P&O MPPT, battery storage governed by an energy-balance and state-of-charge model, and priority-based load scheduling. Because irradiance and module area were not instrumented, efficiency is reported only conditionally and the cost–benefit figures are presented as explicit assumptions. The paper's value lies in the disciplined, end-to-end traceability from a single measured dataset to a deployable EMS concept, and in the concrete list of measurements needed to make the evaluation fully quantitative.

Acknowledgment

The author thanks the laboratory staff for assistance with the experimental setup.

References

[1] M. G. Villalva, J. R. Gazoli, and E. R. Filho, "Comprehensive approach to modeling and simulation of photovoltaic arrays," *IEEE Trans. Power Electron.*, vol. 24, no. 5, pp. 1198–1208, May 2009.

[2] T. Esram and P. L. Chapman, "Comparison of photovoltaic array maximum power point tracking techniques," *IEEE Trans. Energy Convers.*, vol. 22, no. 2, pp. 439–449, Jun. 2007.

[3] M. Kumar et al., "Comprehensive review of conventional and emerging maximum power point tracking algorithms for uniformly and partially shaded solar photovoltaic systems," *IEEE Access*, vol. 11, 2023. DOI: 10.1109/ACCESS.2023.3262502.

[4] M. L. Katche, A. B. Makokha, S. O. Zachary, and M. S. Adaramola, "A comprehensive review of maximum power point tracking (MPPT) techniques used in solar PV systems," *Energies*, vol. 16, no. 5, art. 2206, Mar. 2023. DOI: 10.3390/en16052206.

[5] M. H. Ali, M. Zakaria, and S. El-Tawab, "A comprehensive study of recent maximum power point tracking techniques for photovoltaic systems," *Sci. Rep.*, vol. 15, Apr. 2025. DOI: 10.1038/s41598-025-96247-5.

[6] I. Gomes, K. Bot, M. G. Ruano, and A. Ruano, "Recent techniques used in home energy management systems: A review," *Energies*, vol. 15, no. 8, Apr. 2022. DOI: 10.3390/en15082866.

[7] M. Yousefi, A. Hajizadeh, M. N. Soltani, and B. Hredzak, "Predictive home energy management system with photovoltaic array, heat pump, and plug-in electric vehicle," *IEEE Trans. Ind. Informat.*, vol. 17, no. 1, pp. 430–440, Jan. 2021.

[8] A. Abbasi, H. A. Khalid, R. Habib, and U. K. Adnan, "A novel dynamic load scheduling and peak shaving control scheme in community home energy management system based microgrids," *IEEE Access*, vol. 11, pp. 32508–32522, 2023.

[9] A. Chatterjee, S. Paul, and B. Ganguly, "Multi-objective energy management of a smart home in real time environment," *IEEE Trans. Ind. Appl.*, vol. 59, no. 1, pp. 138–147, Jan./Feb. 2023.

[10] Z. Yi, W. Dong, and A. H. Etemadi, "A unified control and power management scheme for PV-battery-based hybrid microgrids for both grid-connected and islanded modes," *IEEE Trans. Smart Grid*, vol. 9, no. 6, pp. 5975–5985, Nov. 2018.

[11] S. Panda, I. S. Samanta, B. Sahoo, et al., "Comprehensive framework for smart residential demand-side management with electric vehicle integration and advanced optimization techniques," *Sci. Rep.*, vol. 15, art. 9948, 2025.

[12] A. O. Ali, A. M. Hamed, M. M. Abdelsalam, M. N. Sabry, and M. R. Elmarghany, "Energy management of photovoltaic-battery system connected with the grid," *J. Energy Storage*, vol. 55, art. 105865, 2022.